Extremophiles (2011) 15:431–439
DOI 10.1007/s00792-011-0374-3

ORIGINAL PAPER

The characterization of *Thermotoga maritima* ferritin reveals an unusual subunit dissociation behavior and efficient DNA protection from iron-mediated oxidative stress

Pierpaolo Ceci · Elena Forte · Gisa Di Cecca · Manuela Fornara · Emilia Chiancone

Received: 29 December 2010 / Accepted: 31 March 2011 / Published online: 13 April 2011

Abstract Ferritin from the hyperthermophilic anaerobe *Thermotoga maritima*, a bacterium of ancient phylogenetic origin, is structurally similar to known bacterial and eukaryotic ferritins: 24 identical subunits assemble into a shell having octahedral symmetry and a Mr of about 460 kDa. *T. maritima* ferritin (TmFtn), purified to homogeneity as a recombinant protein, contains approximately 2–3 iron atoms and can incorporate efficiently up to 3,500 atoms in the form of a ferric oxy-hydroxide mineral at 80°C, the optimal growth temperature of the bacterium. The 24-mer unexpectedly dissociates reversibly into dimers at low ionic strengths. In turn, dimers re-associate into the native 24-mer assembly at high protein concentrations and upon incorporation of iron micelles containing at least 500 Fe(III). TmFtn uses O_2 as efficient iron oxidant. The reaction stoichiometry is 3–4 O_2:Fe(II) as in all bacterial ferritins. Accordingly no H_2O_2 is released into solution, a feature reflected in the in vitro ability of TmFtn to reduce significantly iron-mediated oxidative damage to DNA at 80°C. A similar TmFtn-mediated ROS detoxifying role likely occurs in the bacterium which lacks the SOD/catalase defense systems of the aerobic world.

Communicated by A. Driessen.

P. Ceci (✉) · E. Chiancone
Institute of Molecular Biology & Pathology, CNR, Rome, Italy
e-mail: pierpaolo.ceci@uniroma1.it

E. Forte · G. Di Cecca · M. Fornara · E. Chiancone (✉)
Department of Biochemical Sciences "A. Rossi Fanelli", Sapienza, University of Rome, P.le A. Moro 5, 00185 Rome, Italy
e-mail: emilia.chiancone@uniroma1.it

Keywords *Thermotoga maritima* ferritin · Subunit association-dissociation properties · Iron incorporation · DNA protection · ROS detoxification

Introduction

Ferritins are ubiquitous proteins that combat the potentially adverse effects of iron in the presence of oxygen (Harrison and Arosio 1996; Chiancone et al. 2004). Thus, Fe(II) potentiates the non-enzymatic production of reactive oxygen species (ROS) while Fe(III), the stable oxidation state, forms at neutral pH values insoluble ferric hydroxide polymers that decrease the bioavailability of this essential metal. Both phenomena are prevented by ferritins whose task is twofold: removal of free Fe(II) from cytoplasm and solubilization of Fe(III). Consequently, the highly conserved ferritin structure is characterized by binuclear ferroxidase centers, which ensure the catalyzed oxidation of Fe(II), and by a shell-like protein assembly that creates a cavity where as many as 4000 iron atoms can be stored in the form of ferric oxy-hydroxide micelles. Importantly, ferritin iron can be released after reduction when the metabolic needs of the organism so require and thus contributes to maintain iron homeostasis (Theil 2004; Arosio et al. 2009).

The ferritin oligomer consists of 24 identical or highly similar subunits folded in four-helix bundles and related by 432 symmetry (Hempstead et al. 1994; Arosio and Levi 2002; Tatur et al. 2007) with the only known exception of *Archaeoglobus fulgidus* ferritin endowed with 23 tetrahedral symmetry (Johnson et al. 2005). In vertebrates, two subunit types can be distinguished, the H-chains (21 kDa), whose ferroxidase center is embedded in the four-helix bundle of single subunits (Lawson et al. 1989), and the

L-chains (20 kDa), which contain nucleation centers for the iron micelles (Harrison and Arosio 1996). In all other organisms the ferritin subunits are alike and of the H-type. Bacteria may also contain the so-called bacterioferritin containing 12 hemes bound at the interface of twofold symmetry related subunits (Hempstead et al. 1994; Andrews 1998) and of still undefined function (Carrondo 2003). The hydrophilic, negatively charged pores that traverse the ferritin oligomer at the junction of threefold symmetry related subunits represent an additional, typical, functionally relevant feature (Yang et al. 2000). The negative electrostatic gradient thus produced attracts Fe(II) and guides it toward the ferroxidase centers. Thereafter, Fe(III) moves to the protein cavity where the iron core nucleates and grows. In vitro, the catalyzed oxidation is complete within seconds, while the hydrolysis-mineralization step, which implies the turnover of metal at the ferroxidase centers, requires minutes (Zhao et al. 2001, 2003).

In ferritins from higher Eukarya two limiting Fe^{2+}/O_2 stoichiometries can be distinguished during the oxidation/uptake process, namely

$$2Fe^{2+} + O_2 + 6H_2O \rightarrow 2Fe(OH)_3 + H_2O_2 + 4H^+ \quad (1)$$

$$4Fe^{2+} + O_2 + 10H_2O \rightarrow 4Fe(OH)_3 + 8H^+ \quad (2)$$

At low iron loading levels, Fe^{2+}/O_2 values near 2.0 are observed, indicative of H_2O_2 formation according to reaction (1). At high iron loading levels, values near 4.0 are measured that point to reduction of O_2 to H_2O by reaction (2). On these bases, reaction (1) was proposed to occur at the ferroxidase centers of native ferritins and of recombinant human H-chain ferritin (HFtHu), while reaction (2) becomes increasingly important during formation of the mineral core (Zhao et al. 2001, 2003). Bacterial ferritins likewise use molecular oxygen to oxidize iron. However, the iron oxidation stoichiometry corresponds to 3–4 $Fe(II)/O_2$ and entails the complete reduction of O_2 to water (Treffry et al. 1998; Bunker et al. 2005). This peculiarity of the iron oxidation process, which results in a significant, highly beneficial reduction in the formation of reactive oxygen species, has been correlated to the presence of a third iron-binding site close to the ferroxidase center (Treffry et al. 1998).

Bacterial ferritins from extremophiles have received relatively little attention. The X-ray crystal structures are limited to the proteins from *A. fulgidus* (AfFtn; PDB ID: 1S3Q), a sulfate-reducing thermophilic anaerobe, *Pyrococcus furiosus* (PfFtn; PDB ID: 2JD6), a strict anaerobe and hyperthermophilic archaeon, and *Thermotoga maritima* (TmFtn; PDB ID: 1VLG), a strict anaerobe, the first known hyperthermophile of bacterial rather than of archaeal origin (Tatur et al. 2007; Johnson et al. 2005; Huber et al. 1986).

T. maritima belongs to a slowly evolving lineage and has an ancient phylogenetic position within the bacterial kingdom, according to macromolecule-based phylogenetic and whole genome-based analyses (Darimont and Sterner 1996; Fitz-Gibbon and House 1999; Nelson et al. 1999). It is an organotrophic bacterium isolated originally from a shallow, geothermally heated marine sediment in the island of Vulcano, Italy. *T. maritima* grows optimally at 80–90°C and at ~0.5 M salt, similar to the salt concentration of seawater, its natural habitat (Huber et al. 1986). Recently, several reports proposed that *Thermotoga*, though a strict anaerobe, has to face temporary oxygen exposure in the hot ecosystems it inhabits and, therefore, must be able to deal with temporary oxidative conditions (Rusch et al. 2005; Van Ooteghem et al. 2004; Eriksen et al. 2008). Another likely problem *T. maritima* has to face is the high concentrations (μM to mM) of free ferrous iron that characterize the geothermally heated marine sediment and might enhance oxygen toxicity. As already mentioned, free Fe(II) potentiates the non-enzymatic ROS production through several reactions which comprise the Fenton reaction ($Fe(II) + H_2O_2 \rightarrow Fe(III) + OH^{\cdot} + OH^-$).

To protect themselves from oxygen toxicity, aerobic organisms have developed specific mechanisms that involve sets of enzymes with different specificities such as superoxide dismutase (Ludwig et al. 1991), catalase (Chance et al. 1979), and nonspecific peroxidases (Ludwig et al. 1991; Ortiz de Montellano 1992). *T. maritima*, like most anaerobes, does not contain catalase, SOD or peroxidases. However, it can combat the damaging action of ROS during the possible, temporary exposure to oxygen as the genome contains genes coding for rubrerythrin, believed to have a peroxidase-like function in other anaerobic bacteria (Coulter et al. 1999), superoxide reductase and a flavodiiron protein (Nelson et al. 1999). The possible participation of ferritin in the defense strategy against ROS is not only of interest per se, given the special phylogenetic position of *T. maritima*, but can provide new insights into the cellular mechanisms used by the first anaerobic forms of life to handle oxidative conditions.

These considerations prompted the present solution study of *T. maritima* ferritin whose properties have never been investigated, despite the availability of the X-ray crystal structure. The protein, obtained in the recombinant form in *E. coli,* is characterized by the reversible dissociation of the 24-mer into dimers at low ionic strengths. This phenomenon does not occur in mammalian ferritins, whose 24-meric assemblage is highly stable (Harrison and Arosio 1996; Arosio et al. 2009), but takes place in *Escherichia coli* bacterioferritin (Andrews et al. 1993). Interestingly, iron oxidation/incorporation induces reassociation of dimers into the canonical 24-mer at low ionic strengths, while leading to formation of highly homogeneous iron

oxide nanoparticles inside the protein cavity. Iron oxidation at the ferroxidase centers takes place efficiently in the presence of O_2 that is reduced directly to H_2O without intermediate H_2O_2 formation. Further, in vitro TmFtn inhibits the release of ROS into solution at 80°C in the presence of H_2O_2 and Fe(II). On this basis it may be surmised that, during the possible exposure of the bacterium to oxygen, TmFtn plays a role in the protection of DNA similarly to other members of the ferritin family, namely the bacterial Dps (DNA-binding proteins from starved cells) proteins (Zhao et al. 2002; Bellapadrona et al. 2010; Chiancone and Ceci 2010).

Materials and methods

Cloning, overexpression and purification of TmFtn

The expression vector pET-11a containing the *TmFtn* gene was purchased from GENEART AG (Germany). Gene synthesis was performed using the TmFtn protein sequence downloaded from the UniProt database (UniProt Consortium 2010, http://www.uniprot.org) and taking into consideration the codon-optimization for high level expression in *Escherichia coli*. The plasmid was introduced into *E. coli* BL21 (DE3) and sequenced by dideoxy sequencing to confirm the presence of the correct gene. *E. coli* BL21 (DE3) cells harboring the recombinant TmFtn plasmid were grown to OD_{600} 0.6 at 37°C in 1 L of ampicillin-containing liquid Luria–Bertani (LB) medium (10 g/L tryptone, 5 g/L yeast extract, and 5 g/L NaCl). Gene expression was induced by addition of 0.5 mM isopropyl thio-β-D-galactoside (IPTG) and the culture was incubated further for 2–3 h. Cells were harvested by centrifugation (15000*g* for 20 min) and suspended in 50 mM Tris–HCl (pH 7.5), 0.5 mM dithiothreitol, 1 mM EDTA, and 500 mM NaCl and disrupted by sonication. The lysate was centrifuged at 15000*g* for 40 min and the supernatant was treated 30 min at 37°C with 0.1 mg/mL DNase (Sigma-Aldrich) supplied with 5 mM $MgCl_2$, heated to 90°C for 10 min, cooled on ice, and then centrifuged to remove denatured proteins. The recovered supernatant was dialyzed overnight against milli-Q water, sterile filtered and stored at 4°C. The purity of all the preparations was assessed using Coomassie brilliant blue staining of 15% PAGE gels run in the presence of SDS. Moreover, the UV/visible spectrum points to the absence of non-protein contaminants. Protein concentration was determined spectrophotometrically at 280 nm using a molar extinction coefficient of 29910 M^{-1} cm^{-1} (ProtParam software, http://www.expasy.org). The iron content of the ferritin samples was assessed by the modified ferrozine method (Percival 1991) that entails reduction of Fe(III) by mercaptoacetic acid and stabilization of the ferrozine–iron complex at acid pH (Fluka).

Analysis of X-ray crystal structure

The amino acid sequence and three-dimensional structure of TmFtn were obtained from the Protein Data Bank (http://www.pdb.org/) (Berman et al. 2000). The structural sequence of TmFtn was produced by SSM (http://www.ebi.ac.uk/msd-srv/ssm/) (Krissinel and Henrick 2004). Structure visualization and analyses were performed using PyMol (Delano Scientific LLC, San Carlos, LA, http://www.pymol.org).

Subunit association/dissociation processes

The state of association of TmFtn was determined by means of size exclusion gel chromatography (SEC) and analytical ultracentrifugation (AUC) experiments as a function of ionic strength. TmFtn samples at 2 mg/mL concentration were applied to a Superose 6 gel-filtration column (GE Healthcare) connected to a GE Healthcare FPLC system (UNICORN) and eluted at a flow rate of 0.5 mL/min at 25°C. The buffer used was 50 mM MOPS-NaOH buffer at pH 7.5 unless otherwise stated. Horse spleen ferritin (450 kDa), *Listeria innocua* Dps (215 kDa), ovalbumin (43 kDa), and myoglobin (16.9 kDa) were run independently under the same conditions to calibrate the column (see inset of Fig. 2). Oligomerization state was determined from the calculated molecular weight and the predicted monomer molecular weight.

Sedimentation velocity study experiments were conducted at 30000 rev/min and 20°C in a Beckman Optima XL-I analytical ultracentrifuge equipped with absorbance optics. Radial absorbance scans were obtained at 280 or 405 nm and at a spacing of 0.003 cm with three averages in a continuous scan mode. Sedimentation coefficients were calculated using the software Sedfit (provided by Dr. P. Schuck, National Institutes of Health) and reduced to water and 20°C ($s_{20,w}$) using standard procedures after calculation of the buffer density and viscosity by the software Sednterp. Sedimentation coefficient distributions, c(s), were obtained using the linear least-squares algorithm (ls-g(s)) incorporated in Sedfit (version 8.3). The molecular mass of the components was calculated assuming a spherical shape and a partial specific volume of 0.736 mL/g.

Iron incorporation experiments

Iron incorporation experiments were carried out at 80°C on 2 mg/mL TmFtn samples in water at a constant pH of 7.0 maintained dynamically with 100 mM NaOH by means of an automatic titrator (TITRINO, Metrohm AG). Solutions

of $FeSO_4$ dissolved in 0.5 mM HCl were used as iron source. Iron (3500 Fe(II)/24-mer) was added to the TmFtn solution aerobically under magnetic stirring by means of a stepwise procedure that entailed successive additions of 100 Fe(II)/24-mer; the time interval between steps was 5 min. The reaction was complete 20 min after the last Fe(II) addition. The final solution was centrifuged at 26000*g* for 20 min, dialyzed overnight against 50 mM MOPS-NaOH buffer at pH 7.5 and analyzed by SEC using a Superose 6 gel-filtration column and by AUC.

Thermostability

Protein thermostability was assessed at 100°C by following the circular dichroism signal at 222 nm to monitor the thermal unfolding process. A Jasco J-715 spectropolarimeter was used; temperature was varied in steps of 1°C/min; the protein, at 1 mg/mL in milli-Q water, was kept in stoppered 0.1 cm quartz cells.

Oxygraphic measurements

Oxygen consumption assays were carried out in a gas-tight vessel using Clark-type selective electrodes (Oxygraph-2K, Oroboros Instruments, Innsbruck, Austria). A ferrous sulfate solution was added to 4 μM recombinant TmFtn or to recombinant human H-ferritin (HFtHu) to achieve a Fe(II)/24-mer molar ratio of 24:1. At the end of the reaction, the possible presence of H_2O_2 was monitored by addition of 2 mg/mL bovine liver catalase (Sigma-Aldrich). Measurements were performed at 25°C in air-equilibrated 20 mM MOPS, pH 7.0. The software DatLab 4.2 furnished by the manufacturers was used for data acquisition and analysis.

DNA protection assays

Two different in vitro assays were set up to assess DNA protection from Fe(II)-mediated oxidative damage. One assay utilizes agarose gel electrophoresis (Zhao et al. 2002; Ceci et al. 2003). In these experiments, the integrity of 20 nM supercoiled pET-11a DNA (5600 bp) was measured at 85°C after exposure to a hydroxyl radicals generating mixture of Fe(II) and H_2O_2. The total reaction volume was 16 μL in 20 mM MOPS-NaOH, pH 7.0; 3 μM TmFtn or bovine serum albumin (BSA) were mixed sequentially with 20 nM pET-11a, 144 μM $FeSO_4$ in 0.5 mM HCl, and 1 mM H_2O_2. Thereafter, the reaction mixture was incubated in 1% SDS at 100°C for 10 min. Plasmid DNA was resolved by electrophoresis on 1% agarose gel in 0.04 M TAE (Tris–Acetic acid-EDTA) buffer at pH 8.5. The gel was stained with ethidium bromide and imaged using ImageMaster VDS (Amersham Biosciences).

The other assay evaluates the iron-dependent hydroxyl radical formation according to the fluorimetric procedure described by Halliwell and Gutteridge (1981) as modified by Ceci et al. (2003). In brief, Fe(II) salts in solution generate hydroxyl radicals that degrade deoxyribose to a malondialdehyde-like compound that forms a fluorescent chromogen with thiobarbituric acid (TBA). The total reaction volume (1.2 mL) contained (final concentrations): potassium phosphate buffer (10 mM, pH 7.4), NaCl (63 mM), deoxyribose (1 mM) and 1 μM TmFtn or BSA. The reaction was initiated by adding $FeSO_4$ (48 μM). After incubation at 85°C for 10 min, TBA (1 mL at 1% w/v) plus trichloracetic acid (1 mL at 2.8% w/v) were added. Thereafter, the mixture was heated at 100°C for 10 min, cooled, and the fluorescence emission of the chromogen measured at 553 nm (λ_{ex} 532 nm) using a Fluoromax fluorimeter (Spex Industry).

Results and discussion

Expression and purification of recombinant ferritin

The ferritin gene from *T. maritima* was cloned and expressed as authentic, functional protein in *E. coli* cells. The overexpressed ferritin accounted for ~40% of the total protein in the cell-free extract (not shown). The stringent heating step at 90°C used for ferritin purification was motivated by the hyperthermostability of *T. maritima*, which grows optimally at about 80°C (Huber et al. 1986). The heating step produced pure protein, based on SDS gel electrophoresis, at typical yields of around 200 mg/L of *E. coli* culture. After purification, all the ferritin samples had very low iron content (2–3 iron atoms per 24-mer) as assessed by the ferrozine assay (Percival 1991).

Quaternary structure

In the X-ray crystal structure (PDB ID: 1VLG), *T. maritima* ferritin displays the canonical quasi-spherical, shell-like assembly with 432 point-group symmetry, formed by 24 identical, 4-helix bundle subunits and traversed by small pores at the 3- and 4-fold symmetry axes (Fig. 1). Hydrophilic, negatively charged residues line the pore entry and create the characteristic negative electrostatic gradient used to guide Fe(II) toward the ferroxidase centers. These possess the iron ligands pertaining to the canonical bi-nuclear ferroxidase centers (Fig. 1), namely E19, E52, H55, E96 and E132, and those creating the additional iron-binding site in its vicinity that is characteristic of bacterial ferritins, namely E51, E128 and E131 as well as E132 (Johnson et al. 2005; Stillman et al. 2001). This particular arrangement of iron ligands provides the

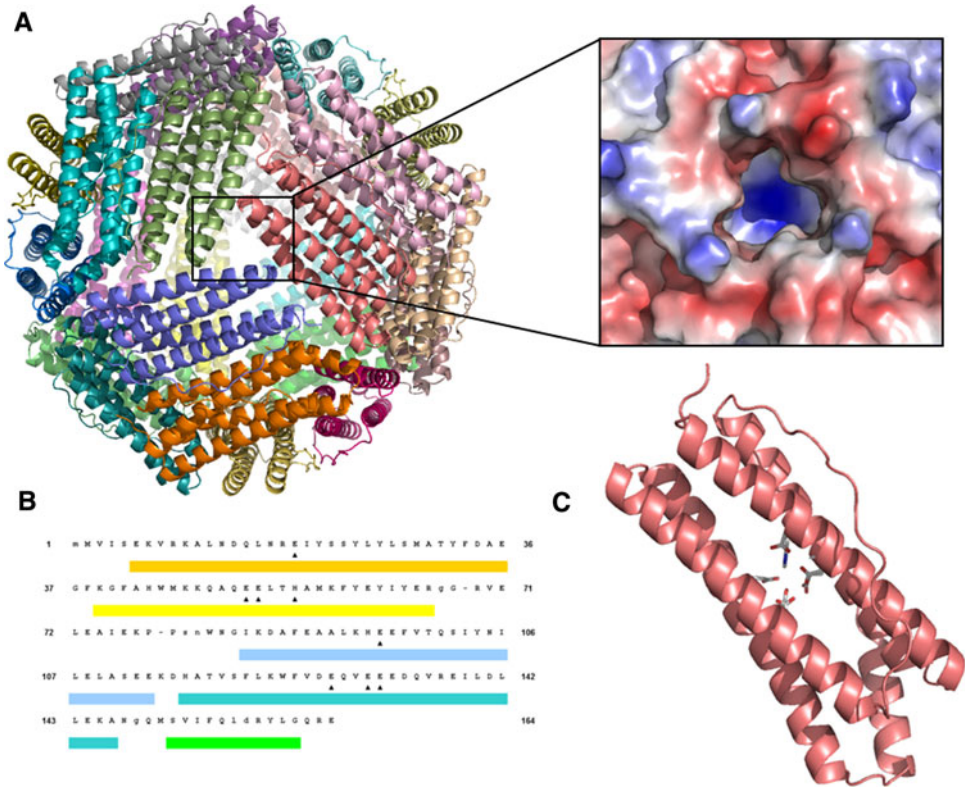

Fig. 1 Structure and sequence of *T. maritima* ferritin. **a** view of TmFtn, a hollow spherical protein composed of 24 subunits, along a threefold symmetry axis. The subunits are shown in *different colors*. In the blow-up, the electrostatic potential surface brings out the negatively charged iron entry into the protein cavity. *Red* indicates negative charges, *blue* positive charges, and *white* neutral charges. **b** the structure-based sequence of TmFtn. α-helices *A–E* are represented as *colored rectangles*. Iron-binding residues at the ferroxidase center and the nearby third iron-binding site are indicated by *black triangles*. **c** a schematic representation of the monomer structure showing the four antiparallel helices, the iron-binding residues at the ferroxidase center and the nearby third iron-binding site. The figure was obtained with Pymol (color figure online)

molecular basis for the capacity of bacterial ferritins to reduce O_2 directly to H_2O without intermediate H_2O_2 production. In the known ferritin X-ray structures the occupancy of these three sites with iron varies. Thus, *E. coli* FtnA (Stillman et al. 2001) and *A. fulgidus* ferritin (Johnson et al. 2005) contain one iron in each of the three sites; *Campylobacter jejuni* ferritin contains two water molecules in place of the iron atoms in the canonical ferroxidase center; TmFtn contains one iron and a water molecule. Based on the conservation of the metal ligands at all three iron-binding sites, TmFtn is expected to oxidize/incorporate iron efficiently like the other bacterial ferritins.

To establish whether the 24-meric assembly is stable in solution, size exclusion gel chromatography (SEC) and analytical ultracentrifugation (AUC) experiments were carried out on the apoprotein under different experimental conditions (Fig. 2; Table 1). The elution profiles display two components (Fig. 2) of about 38 and 440 kDa, two values that match those calculated for dimers and 24-mers from the amino acid composition, respectively 36.0 and 430.0 kDa. This close correspondence indicates that dissociation intermediates are not present to a significant extent. The relative amounts of dimers and 24-mers, obtained by integration of the respective areas using the software Origin 7.5 (Originlab Corporation), have a marked dependence on experimental conditions. Thus, apo-TmFtn exists largely as dimers at the cytoplasmic ionic strengths of moderately halophilic bacteria (Brown 1964)

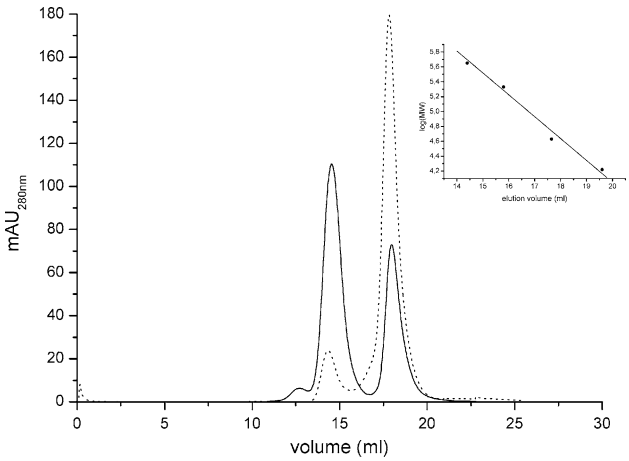

Fig. 2 Association state of apo-TmFtn. Gel-filtration elution profiles of dimeric and 24-meric species. Samples were in 50 mM MOPS-NaOH buffer at pH 7.5 (*dotted line*) or the same buffer supplemented with 0.2 M NaCl (*solid line*). TmFtn elutes as a dimer (17.8 mL; M_w ~ 38 kDa) and as a 24-mer (14.5 mL; M_w ~ 440 kDa). The *inset* shows the calibration curve of the Superose 6 column

and in water, as established also in sedimentation velocity experiments at low protein concentrations.

Several observations demonstrate that the subunit association–dissociation process is reversible. Firstly, the amount of dimers decreases when the initial protein concentration increases from 2 to 20 mg/mL (Table 1). Further, the reversibility of the ionic strength effect is proven

Table 1 Effect of different solution conditions on the association state of *T. maritima* ferritin

Conditions	Method[a]	Dimer (%)	24-mer (%)	Dimer of 24-mer (%)
H_2O_{dd}	AUC	98 ± 1.8	2 ± 1.8	
50 mM MOPS	AUC, SEC	89 ± 2.1	11 ± 2.1	
50 mM MOPS[b]	SEC	78 ± 1.5	22 ± 1.5	
50 mM MOPS, 0.2 M NaCl	AUC, SEC	41 ± 4.5	58 ± 4.5	1
H_2O_{dd}, 14 mM Fe(II) (3500 Fe(II)/24-mer)	AUC, SEC		97 ± 1.6	3 ± 1.6

[a] The association state was evaluated using analytical ultracentrifugation (AUC) and size exclusion gel chromatography (SEC) techniques (see "Materials and methods" for details). The experiments were carried out on three different protein preparations and are reported as mean and standard deviation. Protein concentration was 2 mg/mL in SEC and 0.4 mg/mL in AUC experiments

[b] Protein concentration: 20 mg/mL

by the fact that the 24-mer, isolated after SEC at high ionic strength, dissociates into dimers after dialysis at low ionic strengths (not shown). As mentioned above, *E. coli* Bfn (EcBfn) dissociates into dimers to very much the same extent as TmFtn at pH values around neutrality and 0.15 M NaCl (see Fig. 3 of Andrews et al. 1993); however, the effect of ionic strength and protein concentration on the dissociation process was not studied.

The stability of TmFtn was evaluated also as a function of temperature by monitoring the CD signal in the far-UV CD region (at 220 nm) in water, a condition where only dimers are present in solution at room temperature (Table 1). The constancy of the CD signal even at 100°C points to the absence of a transition from the native to the denatured state and proves the extremely high temperature stability of protein dimers, the building blocks of the fully assembled structure (data not shown).

Iron incorporation experiments

The addition of Fe(II) to apo-TmFtn (3500 atoms/24-mer) was carried out in water at a constant pH of 7.0 and 80°C (see "Materials and methods" for details) to investigate whether the iron incorporation process alters the relative proportion of dimers and 24-mers in solution. Iron incorporation results in the formation of an orange colored solution containing, respectively, ≥95% or 90% of the initial protein. Accordingly, there was no or little precipitate after centrifugation of the solution at the end of the reaction, while bulk precipitation of iron hydroxide polymers occurs in control reactions run in the absence of protein. The formation of protein-enclosed iron nanoparticles was established experimentally by means of SEC experiments. The TmFtn samples were dialyzed versus 50 mM MOPS-NaOH, pH 7.5 and were loaded on a Superose 6 column for analysis. Over 90% of the protein is characterized by the same elution volume of the apo-protein 24-mer (data not shown). Importantly, the same pattern

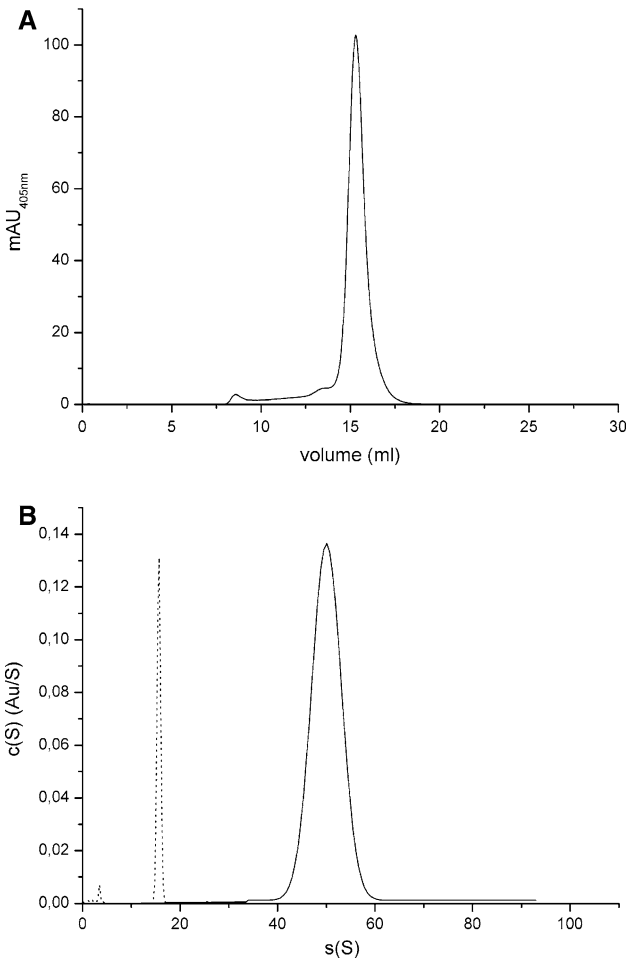

Fig. 3 Gel filtration chromatography and analytical ultracentrifugation of iron-containing TmFtn. **a** Gel-filtration elution profile of TmFtn after oxidation/incorporation of 3500 iron atoms/24-mer in water. **b** Sedimentation coefficient distributions of apoTmFtn before (*dashed line*) and after incorporation of 3500 Fe atoms/24-mer in water (*solid line*)

is obtained at 405 nm, where solely the iron cluster absorbs (Fig. 3a) and at 280 nm, where the protein moiety contributes to the absorbance, proving the composite nature of

the material. The amount of iron in the major peak of the iron-incorporated TmFtn samples was estimated to be 3450 atoms/24-mer, on the basis of the ferrozine assay (Percival 1991) and of quantitative protein assays (Ceci et al. 2010), an indication that essentially all the added iron participates in the formation of protein-enclosed oxide nanoparticles. Analytical ultracentrifugation was used to assess their molecular mass distribution. The sedimentation velocity (Fig. 3b) of the TmFtn sample incorporated in water (50 S) is in good agreement with the estimated $s_{20,w}$ value of a ferritin molecule containing ~3500 Fe atoms/24-mer (May et al. 2010). It is worth highlighting that the ferric nanoparticles are characterized by a relatively small degree of polydispersity even though the starting solution contained mainly TmFtn dimers. This fact lends itself to be exploited in the nano-biotechnological area given the well-known strong dependence of the properties of nanoparticles on their size and homogeneity.

To our knowledge, a role of iron micelles in the stabilization of the ferritin assemblage has never been observed in canonical ferritins, with the only exception of the unusual *A. fulgidus* protein after incorporation of 500 Fe/24-mer (Johnson et al. 2005).

Oxygraphic measurements

The iron oxidation reaction was characterized further in oxygraphic experiments to establish the stoichiometry and the possible presence of H_2O_2 in solution at the end of the reaction. Solutions of Fe(II) were added to 4 μM TmFtn or HFtHu to achieve a molar ratio of 24 Fe atoms/24-mer and oxygen consumption was measured. The addition of Fe(II) results in fast oxygen consumption according to O_2:Fe(II) molar ratios of 1:3 in TmFtn and 1:2 in HFtHu (Fig. 4). The significance of this difference is proven by the addition of catalase at the end of the reaction. Catalase does not cause O_2 formation in the presence of TmFtn indicating that H_2O_2 is not released into solution. In contrast, catalase leads to O_2 formation in the presence of HFtHu, where the ferroxidation reaction is known to result in the quantitative production of H_2O_2 according to reaction (1). In this connection it should be mentioned that TmFtn can use H_2O_2 as well as molecular oxygen to oxidize Fe(II) like the other bacterial ferritins (Bunker et al. 2005) and Dps proteins (Zhao et al. 2002).

These findings show that TmFtn reduces O_2 directly to H_2O without intermediate H_2O_2 formation, in accordance with the foreseen existence of a third Fe binding site close to the ferroxidase center as in all known bacterial ferritins. On this basis, TmFtn might prevent formation of reactive oxygen species. To test this hypothesis, the ability of TmFtn to prevent DNA cleavage mediated by hydroxyl radicals was determined by means of in vitro assays.

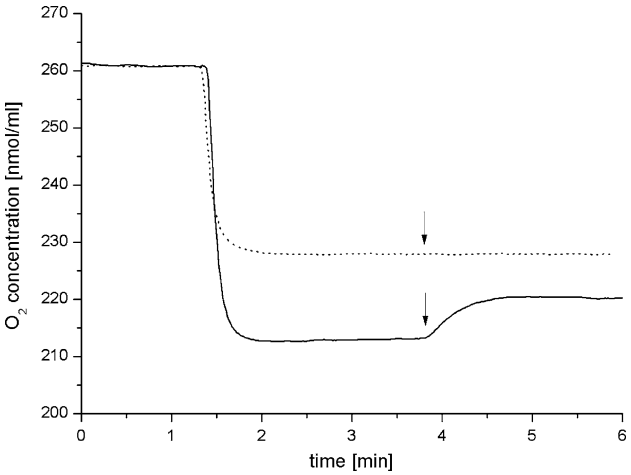

Fig. 4 Oxygen consumption during Fe(II) oxidation in the presence of TmFtn or recombinant human H-ferritin (HFtHu). A solution of Fe(II) was added (at 80 s) to 4 μM TmFtn (*dotted line*) or HFtHu (*solid line*) at a molar ratio of 24 Fe(II)/24-mer. Buffer: 20 mM MOPS-NaOH pH 7.0, at 25°C. The addition of Fe(II) to both TmFtn and HFtHu results in fast oxygen consumption according to the O_2:Fe(II) molar ratios of 1:3 or 1:2, respectively. The subsequent addition of catalase (*arrows*) results in oxygen production only in the case of HFtHu

ROS formation assays

In one type of assay, plasmid pET-11a DNA in 20 mM MOPS-NaOH, pH 7.0 was exposed to hydroxyl radicals formed via Fenton chemistry by the combined effect of H_2O_2 and Fe(II) in a molar ratio of 48 atoms/24-mer. Plasmid DNA alone is fully degraded as shown by comparison of lanes 1 and 3 in Fig. 4. In the presence of TmFtn hydroxyl radicals are not formed and efficient DNA protection is achieved, as indicated by the essentially unaltered pattern of the plasmid bands (Fig. 4, lanes 1 and 2). In contrast, BSA used as control does not afford protection and DNA is degraded entirely (Fig. 4, lane 4).

In the other type of experiment, the capacity of TmFtn and BSA to inhibit the Fe(II)-dependent hydroxyl radical formation was investigated using the fluorimetric assay described under "Materials and methods" (Ceci et al. 2003). The presence of TmFtn prevents hydroxyl radical formation efficiently since the extent of inhibition was 79 ± 3%. In contrast, BSA has practically no inhibitory effect (5 ± 4% inhibition).

These results substantiate the oxygraphic data and point to a potential role of TmFtn in the protection of the bacterium under the conditions of temporary oxidative stress it may encounter (Fig. 5).

Conclusions

The association–dissociation behavior and functional properties of recombinant ferritin from the hyperthermophilic

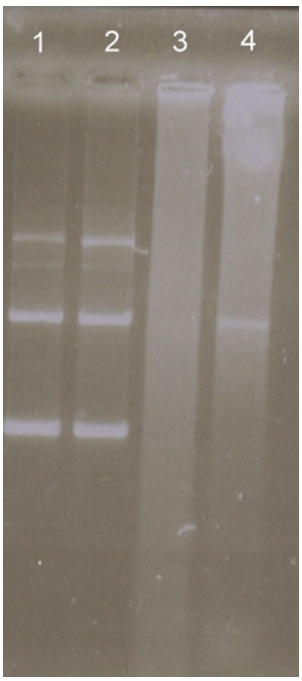

Fig. 5 ROS formation in the presence of TmFtn as monitored in a DNA protection assay. *Lane 1*, plasmid DNA; *lane 2*, plasmid DNA with 1 mM H_2O_2, 144 μM Fe(II) and 3 μM TmFtn; *lane 3*, plasmid DNA with 1 mM H_2O_2, 144 μM Fe(II); *lane 4*, plasmid DNA with 1 mM H_2O_2, 50 μM Fe(II) and 3 μM BSA. Conditions: agarose gel (1%) in 0.04 M TAE (Tris–Acetic acid-EDTA) buffer at pH 8.5

obligate anaerobe *T. maritima* are of interest from several perspectives. The reversible dissociation of the TmFtn 24-mer into dimers at low ionic strengths, and the observation that subunit re-association is promoted by formation of iron micelles in the internal cavity provide insight into structure–function relationships within the ferritin family and in addition lend themselves to be exploited in the production of nano-sized material for chemical, physical and biomedical applications, an area of active research (Uchida et al. 2008; Kasyutich et al. 2008, 2010; Ueno et al. 2004; Turyanska et al. 2009; Prastaro et al. 2009).

Among the family members, to date only *E. coli* bacterioferritin has been shown to dissociate under quasi-physiological conditions. In terms of function, the efficiency of iron oxidation/uptake at 80°C and the characteristics of the ferroxidation reaction, which takes place without the intermediate production of H_2O_2, are of value in connection with the mechanisms used by the first anaerobic forms of life, which possess rubrerythrin, but lack the catalase/SOD systems, to combat oxidative stress during temporary exposure to oxygen.

Acknowledgments PNRA and local MIUR funds to EC are gratefully acknowledged.

References

Andrews SC (1998) Iron storage in bacteria. Adv Microb Physiol 40:281–351

Andrews SC, Smith JM, Hawkins C, Williams JM, Harrison PM, Guest JR (1993) Overproduction, purification and characterization of the bacterioferritin of *Escherichia coli* and a C-terminally extended variant. Eur J Biochem 213:329–338

Arosio P, Levi S (2002) Ferritin, iron homeostasis, and oxidative damage. Free Radic Biol Med 33:457–463

Arosio P, Ingrassia R, Cavadini P (2009) Ferritins: a family of molecules or iron storage, antioxidation and more. Biochim Biophys Acta 1790:589–599

Bellapadrona G, Ardini M, Ceci P, Stefanini S, Chiancone E (2010) Dps proteins prevent Fenton-mediated oxidative damage by trapping hydroxyl radicals within the protein shell. Free Radic Biol Med 48:292–297

Berman HM, Westbrook J, Feng Z, Gilliland G, Bhat TN, Weissig H et al (2000) The Protein Data Bank. Nucleic Acids Res 28:235–242

Brown AD (1964) Aspects of bacterial response to the ionic environment. Bacteriol Rev 28:296–329

Bunker J, Lowry T, Davis G, Zhang B, Brosnahan D, Lindsay S, Costen R, Choi S, Arosio P, Watt GD (2005) Kinetic studies of iron deposition catalyzed by recombinant human liver heavy, and light ferritins and *Azotobacter vinelandii* bacterioferritin using O_2 and H_2O_2 as oxidants. Biophys Chem 114:235–244

Carrondo MA (2003) Ferritins, iron uptake and storage from the bacterioferritin viewpoint. EMBO J 22:1959–1968

Ceci P, Ilari A, Falvo E, Chiancone E (2003) The Dps protein of *Agrobacterium tumefaciens* does not bind to DNA but protects it toward oxidative cleavage: x-ray crystal structure, iron binding, and hydroxyl-radical scavenging properties. J Biol Chem 278:20319–20326

Ceci P, Chiancone E, Kasyutich O, Bellapadrona G, Castelli L, Fittipaldi M, Gatteschi D, Innocenti C, Sangregorio C (2010) Synthesis of iron oxide nanoparticles in *Listeria innocua* Dps (DNA-binding protein from starved cells): a study with the wild-type protein and a catalytic centre mutant. Chemistry 16:709–717

Chance B, Sies H, Boveris A (1979) Hydroperoxide metabolism in mammalian organs. Physiol Rev 59:527–605

Chiancone E, Ceci P (2010) The multifaceted capacity of Dps proteins to combat bacterial stress conditions: Detoxification of iron and hydrogen peroxide and DNA binding. Biochim Biophys Acta 1800:798–805

Chiancone E, Ceci P, Ilari A, Ribacchi F, Stefanini S (2004) Iron and proteins for iron storage and detoxification. Biometals 17:197–202

Coulter ED, Shenvi NV, Kurtz DM Jr (1999) NADH peroxidase activity of rubrerythrin. Biochem Biophys Res Commun 255:317–323

Darimont B, Sterner R (1996) Sequence, assembly and evolution of a primordial ferredoxin from *Thermotoga maritima*. EMBO J 13:1772–1781

Eriksen NT, Nielsen TM, Iversen N (2008) Hydrogen production in anaerobic and microaerobic *Thermotoga neapolitana*. Biotechnol Lett 30:103–109

Fitz-Gibbon ST, House CH (1999) Whole genome-based phylogenetic analysis of free-living microorganisms. Nucleic Acids Res 27:4218–4222

Halliwell B, Gutteridge JM (1981) Formation of thiobarbituric-acid-reactive substance from deoxyribose in the presence of iron salts: the role of superoxide and hydroxyl radicals. FEBS Lett 128:347–352

Harrison PM, Arosio P (1996) The ferritins: molecular properties, iron storage function and cellular regulation. Biochim Biophys Acta 1275:161–203

Hempstead PD, Hudson AJ, Artymiuk PJ, Andrews SC, Banfield MJ, Guest JR, Harrison PM (1994) Direct observation of the iron binding sites in a ferritin. FEBS Lett 350:258–262

Huber R, Langworthy TA, Konig H, Thomm M, Woese CR, Sleytr UB, Stetter KO (1986) *Thermotoga maritima* sp. nov. represents a new genus of unique extremely thermophilic eubacteria growing up to 90°C. Arch Microbiol 144:324–333

Johnson E, Cascio D, Sawaya MR, Gingery M, Schröder I (2005) Crystal structures of a tetrahedral open pore ferritin from the hyperthermophilic archaeon *Archaeoglobus fulgidus*. Structure 13:637–648

Kasyutich O, Sarua A, Schwarzacher W (2008) Bioengineered magnetic crystals. J Phys D Appl Phys 41:134022

Kasyutich O, Ilari A, Fiorillo A, Tatchev D, Hoell A, Ceci P (2010) Silver ion incorporation and nanoparticle formation inside the cavity of *Pyrococcus furiosus* ferritin: structural and size-distribution analyses. J Am Chem Soc 132:3621–3627

Krissinel E, Henrick K (2004) Secondary-structure matching (SSM), a new tool for fast protein structure alignment in three dimensions. Acta Cryst D60:2256–2268

Lawson DM, Treffry A, Artymiuk APJ, Harrison PM, Yewdall SJ, Luzzago A, Cesareni G, Levi S, Arosio P (1989) Identification of the ferroxidase centre in ferritin. FEBS Lett 254:207–210

Ludwig ML, Metzger AL, Pattridge KA, Stallings WC (1991) Manganese superoxide dismutase from *Thermus thermophilus*. A structural model refined at 1.8 Å resolution. J Mol Biol 219:335–358

May CA, Grady JK, Laue TM, Poli M, Arosio P, Chasteen ND (2010) The sedimentation properties of ferritins. New insights and analysis of methods of nanoparticle preparation. Biochim Biophys Acta 1800:858–870

Nelson KE, Clayton RA, Gill SR, Gwinn ML, Dodson RJ, Haft DH, Hickey EK, Peterson JD, Nelson WC, Ketchum KA, McDonald L, Utterback TR, Malek JA, Linher KD, Garrett MM, Stewart AM, Cotton MD, Pratt MS, Phillips CA, Richardson D, Heidelberg J, Sutton GG, Fleischmann RD, Eisen JA, White O, Salzberg SL, Smith HO, Venter JC, Fraser CM (1999) Evidence for lateral gene transfer between Archaea and Bacteria from genome sequence of *Thermotoga maritima*. Nature 399:323–329

Ortiz de Montellano PR (1992) Catalytic sites of hemoprotein peroxidases. Annu Rev Pharmacol Toxicol 32:89–107

Percival MD (1991) Human 5-lipoxygenase contains an essential iron. J Biol Chem 266:10058–10061

Prastaro A, Ceci P, Chiancone E, Boffi A, Cirilli R, Colone M, Fabrizi G, Stringaro A, Cacchi S (2009) Suzuki-Miyaura cross-coupling catalyzed by protein-stabilized palladium nanoparticles under aerobic conditions in water: application to a one-pot chemoenzymatic enantioselective synthesis of chiral biaryl alcohols. Green Chem 11:1929–1932

Rusch A, Walpersdorf E, deBeer D, Gurrieri S, Amend JP (2005) Microbial communities near the oxic/anoxic interface in the hydrothermal system of Vulcano Island, Italy. Chem Geol 224:169–182

Stillman TJ, Hempstead PD, Artymiuk PJ, Andrews SC, Hudson AJ, Treffry A, Guest JR, Harrison PM (2001) The high-resolution X-ray crystallographic structure of the ferritin (EcFtnA) of *Escherichia coli*; comparison with human H ferritin (HuHF) and the structures of the Fe(3+) and Zn(2+) derivatives. J Mol Biol 307:587–603

Tatur J, Hagen WR, Matias PM (2007) Crystal structure of the ferritin from the hyperthermophilic archaeal anaerobe *Pyrococcus furiosus*. J Biol Inorg Chem 12:615–630

Theil EC (2004) Iron, ferritin, and nutrition. Annu Rev Nutr 24:327–343

Treffry A, Zhao Z, Quail MA, Guest JR, Harrison PM (1998) How the presence of three iron binding sites affects the iron storage function of the ferritin (EcFtnA) of *Escherichia coli*. FEBS Lett 432:213–218

Turyanska L, Bradshaw TD, Sharpe J, Li M, Mann S, Thomas NR, Patanè A (2009) The biocompatibility of apoferritin-encapsulated PbS quantum dots. Small 5:1738–1741

Uchida M, Terashima M, Cunningham CH, Suzuki Y, Willits DA, Willis AF, Yang PC, Tsao PS, McConnell MV, Young MJ, Douglas T (2008) A human ferritin iron oxide nano-composite magnetic resonance contrast agent. Magn Reson Med 60:1073–1081

Ueno T, Suzuki M, Goto T, Matsumoto T, Nagayama K, Watanabe Y (2004) Size-selective olefin hydrogenation by a Pd nanocluster provided in an apo-ferritin cage. Angew Chem Int Ed Engl 43:2527–2530

UniProt Consortium (2010) The Universal Protein Resource (UniProt) in 2010. Nucleic Acids Res 38:D142–D148

van Ooteghem SA, Jones A, van der Lelie D, Dong B, Mahajan D (2004) H_2 production and carbon utilization by *Thermotoga neapolitana* under anaerobic and microaerobic growth conditions. Biotechnol Lett 26:1223–1232

Yang X, Arosio P, Chasteen ND (2000) Molecular diffusion into ferritin. Pathways, temperature dependence, incubation time and concentration effects. Biophys J 78:2049–2059

Zhao G, Bou-Abdallah F, Yang X, Arosio P, Chasteen ND (2001) Is hydrogen peroxide produced during iron(II) oxidation in mammalian apoferritins? Biochemistry 40:10832–10838

Zhao G, Ceci P, Ilari A, Giangiacomo L, Laue TM, Chiancone E, Chasteen ND (2002) Iron and hydrogen peroxide detoxification properties of DNA-binding protein from starved cells. A ferritin-like DNA-binding protein of *Escherichia coli*. J Biol Chem 277:27689–27696

Zhao G, Bou-Abkallah F, Arosio P, Levi S, Janus-Chandler C, Chasteen ND (2003) Multiple pathways for mineral core formation in mammalian apoferritin. The role of hydrogen peroxide. Biochemistry 42:3142–3150